



Perovskite-type LaFeO₃ nanoparticles prepared by thermal decomposition of the La[Fe(CN)₆].5H₂O complex: A new reusable catalyst for rapid and efficient reduction of aromatic nitro compounds to arylamines with propan-2-ol under microwave irradiation

Saeid Farhadi*, Firouzeh Siadatnasab

Department of Chemistry, Lorestan University, Khoramabad 68135-465, Iran

ARTICLE INFO

Article history:

Received 16 November 2010
Received in revised form 16 February 2011
Accepted 3 March 2011

Keywords:

Perovskite-type LaFeO₃
Nanoparticles
Reduction
Nitro compounds
Microwave irradiation

ABSTRACT

Perovskite-type LaFeO₃ nanoparticles were readily synthesized via thermal decomposition of the La[Fe(CN)₆].5H₂O complex and characterized by using thermal analysis (TGA), X-ray diffraction (XRD), Fourier-transformed infrared spectroscopy (FT-IR), scanning electron microscopy (SEM), energy-dispersive X-ray spectroscopy (EDX), transmission electron microscopy (TEM) and BET specific surface area measurement. This nanosized perovskite-type oxide with an average particle size of 35 nm and a specific surface area 38.5 m²/g was used as a new reusable heterogeneous catalyst for highly efficient and selective reduction of aromatic nitro compounds into their corresponding amines by using propan-2-ol as the hydrogen donor under microwave irradiation. This method is regio- and chemoselective, clean, inexpensive and compatible with the substrates having hydrogenlysable or reducible functional groups. As compared with conventional heating, this method is very fast and suitable for large scale preparation of different substituted anilines as well as other arylamines. The catalyst can also be reused without observable loss of its activity.

© 2011 Elsevier B.V. All rights reserved.

1. Introduction

Aromatic amines are a class of the useful organic materials due to their applications in the manufacture of dyestuffs, pharmaceutical products, agricultural chemicals, surfactants and polymers [1,2]. The preparation of aromatic amines is traditionally performed through the reduction of aromatic nitro compounds using catalytic hydrogenation [3] and metallic reagents in acidic media [4–6].

In recent years, numerous new reagents have been developed for the reduction of aromatic nitro compounds to their corresponding amines [7–30]. Among them, catalytic transfer hydrogenation using safe, clean and stable hydrogen donors such as hydrazine hydrate, formic acid and propan-2-ol rather than highly flammable hydrogen gas is one of the most suitable method [31]. This method has potential advantages, including operational simplicity, high selectivity and yield, no highly diffusible and flammable H₂ gas used and no special equipment required. Pt, Pd, Ru and Raney Ni are classical catalysts employed in catalytic transfer hydrogenation [32]. However, expensive metals such as palladium or platinum on carbon and Raney nickel used for this purpose are flammable

when exposed to air and, in most cases, the use of an inert atmosphere is necessary. Since this transformation requires catalysts with high surface area and high acidic active sites, it seems that nanosized materials which possess such characteristics to be suitable for this purpose. Nanostructured catalysts such as silicate or aluminophosphate molecular sieve-supported transition metal ions [33–40], polymer-supported amorphous Ni–B nanoparticles [41] silica-supported gold nanoparticles [42], Mg–Fe hydrotalcite [43], Faujasite NaY zeolite [44] have been employed in the catalytic transfer hydrogenation of nitroarenes. However, these reactions are usually conducted under refluxing conditions, a process that requires several hours of time. Furthermore, the activity of most of these catalysts decreases with subsequent recycling.

Nanostructured transition metal oxides have attracted great interest in recent years due to their particular physical and chemical properties compared to bulk materials [45,46]. Among them, perovskite-type mixed oxides (ABO₃) are promising catalytic materials for the organic transformations due to thermal stability, high resistant to dissolution in aqueous and non-aqueous solutions, and their much lower cost as compared to noble metals [47–53]. The major drawback of traditional perovskite-type oxides is low surface area (≤ 5 m²/g) that limits their catalytic performance. One approach to overcome this problem is to prepare the perovskite-type oxides with nanosized particles. The preparation of nanosized

* Corresponding author. Tel.: +98 6612202782; fax: +98 6616200088.
E-mail address: sfarhad2001@yahoo.com (S. Farhadi).

perovskite-type oxides with sufficiently high surface areas by conventional method since it involves a solid-state reaction of the simple oxides at high temperatures ($\geq 1000^\circ\text{C}$), leading to bulk particles with low-surface-area ($\leq 5\text{ m}^2/\text{g}$). The solid-state thermal decomposition of heteronuclear complexes is one of the simplest and lowest-cost techniques for preparing pure and nanosized perovskite-type oxides with relatively high specific surface area [54]. In fact, the heteronuclear complexes are solid solutions that contain the cations mixed together, essentially on an atomic scale. Because of the high degree of homogenization, much lower temperatures are sufficient for the reaction to occur. This method exhibits many advantages; no need for solvent, surfactant and complex apparatus, high yield, low energy consumption and simple reaction technology.

In continuation of our interest in exploring nanostructured catalysts for organic transformations [55–58], in this work, perovskite-type LaFeO_3 nanoparticles were easily prepared via thermal decomposition of the $\text{La}[\text{Fe}(\text{CN})_6]\cdot 5\text{H}_2\text{O}$ complex and their catalytic activity were evaluated in the reduction of aromatic nitro compounds with 2-propanol as a hydrogen donor under microwave irradiation (MWI). The results indicate that the nanosized perovskite-type LaFeO_3 oxide is a highly selective and efficient recyclable catalyst for the rapid reduction of aromatic nitro compounds to the corresponding amines under MWI. To the best of our knowledge, this is the first report of catalytic reduction of aromatic nitro compounds over a nanosized perovskite-type oxide in conjunction with MWI.

2. Experimental

2.1. Catalyst preparation

$\text{La}[\text{Fe}(\text{CN})_6]\cdot 5\text{H}_2\text{O}$ complex was synthesized as a reddish-brown precipitate via mixing aqueous solutions of equimolar amounts of $\text{La}(\text{NO}_3)_3\cdot 6\text{H}_2\text{O}$ and $\text{K}_3[\text{Fe}(\text{CN})_6]$ with continuous stirring, according to the literature method [54]. The resulting precipitate was washed with water, ethanol and diethyl ether, before drying in air at 50°C . In order to prepare LaFeO_3 nanoparticles, $\text{La}[\text{Fe}(\text{CN})_6]\cdot 5\text{H}_2\text{O}$ (5 g) was placed in a porcelain crucible and was then heated in a furnace electric at 700°C . The temperature for the decomposition of the complex was selected from the result of thermogravimetric analysis (TGA). The decomposition product was cooled to room temperature and collected for the characterization.

In a similar manner above, other nanosized perovskite-type oxides (LnMO_3 ; $\text{Ln} = \text{La, Sm, Nd, Gd, M} = \text{Fe, Co, Cr, Mn}$) have been prepared via the decomposition of their heteronuclear hexacyano complex, $\text{Ln}[\text{M}(\text{CN})_6]\cdot n\text{H}_2\text{O}$. Also, a bulk LaFeO_3 sample was prepared by traditional solid state reaction of La_2O_3 and Fe_2O_3 at temperature of 1000°C after a long heating time of 5 h. The catalytic activity of these samples was compared with the nanosized LaFeO_3 catalyst.

2.2. Catalyst characterization

The nanosized LaFeO_3 catalyst was characterized by using a Bruker D4 Advance X-ray diffractometer with $\text{Cu K}\alpha$ radiation ($\lambda = 1.5405\text{ \AA}$). Thermal analysis (TG) of precursor complex was performed in air atmosphere using a Netzsch STA 409 PC thermal analyzer at a heating rate of $10^\circ\text{C}/\text{min}$. The FT-IR spectra of the samples were recorded on a Shimadzu system FT-IR 160 spectrophotometer using KBr pellets. The powder morphology was observed by a Philips XL-30 scanning electron microscope (SEM) equipped with a link energy-dispersive X-ray (EDX) analyzer. The particle size was determined by a LEO-912AB transmission electron microscope (TEM) at an accelerating voltage of 80 kV. TEM samples

were prepared by dropping the ethanol dispersion on a carbon-coated copper grid. Specific surface area was calculated by the BET method using N_2 adsorption–desorption experiments carried out at -196°C on a Micromeritics ASAP 2010. Before each measurement, the sample was degassed at 150°C for 1 h.

2.3. Catalytic tests

To a solution of nitro compounds (5 mmol) in alcohol (20 mL), KOH pellets (5 mmol) were added along with an appropriate amount of perovskite-type ABO_3 catalyst. The reaction mixture was placed in a 100 mL round-bottomed Pyrex flask equipped with a condenser and was irradiated in a laboratory microwave oven at 180 W for an appropriate time depending upon the nature of the substrate. The progress of the reaction was monitored by TLC and GC–MS. After completion of the reaction, the mixture was cooled to room temperature and the catalyst was filtered off for recycling tests. The filtrate was concentrated under a reduced pressure. The residue was subjected to silica-gel plate chromatography using carbon tetrachloride-ethyl acetate as an eluent to give pure product. Similar experiments have been conducted for studying the effect of catalyst loadings and alcoholic H-donors on the reaction. The results of these experiments are summarized in Tables 1 and 2. The general results are shown in Table 3. In this Table, the products are commercially available and were identified through comparison of their physical and spectral data (mp, FT-IR, ^1H NMR and GC–MS) with those of authentic samples or reported data.

In order to make a comparison, the microwave-assisted catalytic reduction of some nitro substrates was also carried out in the presence of a bulk- LaFeO_3 catalyst and nanosized perovskite-type oxides such as SmFeO_3 , NdFeO_3 , GdFeO_3 , BiFeO_3 , LaCoO_3 , LaCrO_3 and LaMnO_3 under the same reaction conditions as described above. The results are compared in Tables 4 and 5. Also, the reduction of several nitro substrates was conducted under the conventional heating in a similar manner outlined above except that the reaction mixture was refluxed for the appropriate time in an oil-bath rather than microwave irradiation. The results are compared in Table 6.

2.4. Recycling of the catalyst

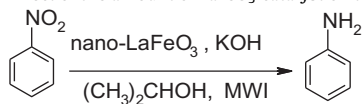
At the end of the reduction of nitrobenzene, the catalyst was filtered, washed with acetonitrile, dried and activated at 200°C for 1 h, and reused in another reaction. The results for five runs are summarized in Table 7.

3. Results and discussion

3.1. Characterization of LaFeO_3 nanoparticles

The thermal decomposition of heteronuclear complexes is a promising method for obtaining pure and nanosized mixed oxides with relatively high specific surface area for catalytic purposes. In this work, the heteronuclear cyano complex, $\text{La}[\text{Fe}(\text{CN})_6]\cdot 5\text{H}_2\text{O}$, as the precursor of perovskite-type LaFeO_3 , was synthesized at room temperature by mixing aqueous solutions of $\text{La}(\text{NO}_3)_3\cdot 6\text{H}_2\text{O}$ and $\text{K}_3\text{Fe}(\text{CN})_6$ under continuous stirring, according to the following reaction: $\text{La}(\text{NO}_3)_3(\text{aq}) + \text{K}_3[\text{Fe}(\text{CN})_6](\text{aq}) \rightarrow \text{La}[\text{Fe}(\text{CN})_6]\cdot 5\text{H}_2\text{O}(\text{s}) + 3\text{KNO}_3(\text{aq})$. First, thermal behavior of the $\text{La}[\text{Fe}(\text{CN})_6]\cdot 5\text{H}_2\text{O}$ complex was studied by thermal analysis. From TGA curve in Fig. 1, two major weight losses are observed. The first weight loss is attributed to the loss of five molecules of crystallization water, whereas second one is due to the decomposition of the cyanide groups which followed by a gradual weight loss until 650°C . The total weight loss is about 44%, which is close to the theoretical value for the formation of

Table 1
Effect of the amount of LaFeO₃ catalyst on the reduction of nitrobenzene with 2-propanol.^{a,b}



Entry	LaFeO ₃ (mol %)	Time (min)	Conversion (%) ^c	Yield (%) ^d
1	1	35	19	14
2	2.5	35	63	56
3	5	18	100	95
4	7.5	20	100	94
5	10	18	100	95
6 ^e	0	25	0	0
7 ^f	5	25	0	0
8 ^g	5	25	0	0

^a Reaction conditions: nitrobenzene (5 mmol), KOH (5 mmol), propan-2-ol (20 mL), under microwave irradiation.

^b In all cases, selectivity was over 99% determined by GC–MS analysis of the crude product mixture.

^c Conversions were determined by GC–MS analysis of the reaction mixture.

^d Yields are for isolated pure product.

^e The reaction was carried out without catalyst.

^f The reaction was carried out without KOH.

^g The reaction was carried out in the absence of microwave irradiation.

Table 2
Effect of the various alcoholic H-donors on the reduction of nitrobenzene.^{a,b}

Entry	H-donor	Time (min)	Conversion (%) ^c	Yield (%) ^d
1	Propan-2-ol	18	100	95
2	Methanol	35	47	40
3	Ethanol	20	94	86
4	Propan-1-ol	35	45	38
5	Butan-2-ol	35	18	12
6	<i>tert</i> -Butyl alcohol	40	0	0

^a Reaction conditions: nitrobenzene (5 mmol), KOH (5 mmol), catalyst (5 mol%), alcohol (20 mL), under microwave irradiation.

^b In all cases, selectivity was over 99% determined by GC–MS analysis of the crude product mixture.

^c Conversions were determined by GC–MS analysis of the reaction mixture.

^d Isolated yields.

LaFeO₃. This finding suggests that the decomposition reaction of the La[Fe(CN)₆].5H₂O complex is completed at about 650 °C. Therefore, we selected 700 °C as the final calcination temperature for the preparation of pure LaFeO₃ nanoparticles.

Fig. 2 shows the XRD pattern of the obtained powder from the decomposition of La[Fe(CN)₆].5H₂O precursor at 700 °C. The recorded diffraction peaks are well assigned to the perovskite-type LaFeO₃ structure (JCPDS File No. 05–0669). No characteristic XRD peaks of phases such as La(OH)₃, La₂O₃, La₂O₂CO₃, Fe₂O₃, Fe₃O₄ and unreacted precursor were observed, indicating the preparation of pure single-phase LaFeO₃ by this method. The average particle size is calculated by using the Debye–Scherrer equation [59]: $d = (0.9\lambda) / (h_{1/2} \cos \theta)$, where d represents the grain size; λ is the wavelength of the X-ray; θ is the diffraction angle of the peak; and $h_{1/2}$ stands for the full-width at half-height of the peaks. The average particle size calculated by the Debye–Scherrer equation was 35 nm which is in accordance with TEM observation (vide infra).

The FT-IR spectra of La[Fe(CN)₆].5H₂O and its decomposition product are shown in Fig. 3. The FT-IR spectrum of the starting complex in Fig. 3(a) shows the characteristic C≡N stretching bands at about 2150, 2060 cm⁻¹ [60]. Also, the bands at 3500 and 1640 cm⁻¹ are related to the stretching and bending vibrations of the lattice water molecules, respectively. As can be seen in the FT-IR spectrum of the product in Fig. 3(b), all of these bands were disappeared after thermal decomposition of the precursor complex at 700 °C. In the FT-IR of the product, the strong bands at about 560 and 440 cm⁻¹ are assigned to the Fe–O stretching and bending vibrations of the octahedral FeO₆ groups in the perovskite-type structure, respectively [61].

It is well-known that the catalytic activity of ABO₃ perovskite-type oxides is strongly dependent on the shape and sizes of their particles. The shape and sizes of LaFeO₃ particles were observed by SEM and TEM. The SEM micrograph of the product powder in Fig. 4(a) clearly shows that the LaFeO₃ powder was formed from strongly aggregated very fine spherical particles. The particles have spherical morphology with a uniform shape. TEM image of the obtained perovskite-phase LaFeO₃ powder is shown in Fig. 4(b). TEM sample was prepared with the dispersion of powder in ethanol by ultrasonic vibration. As can be seen, the powder comprises spherical nanoparticles with a narrow size distribution in the range of 15–60 nm. This is consistent with the average size obtained from the peak broadening in X-ray diffraction studied. Such consistence implies that the LaFeO₃ nanoparticles are single-phase.

The LaFeO₃ product was also tested by EDX analysis. The EDX spectrum of the sample shows peaks of La and Fe elements (Fig. 5). The atomic percentages of La and Fe determined by EDX were 50.18% and 49.82%, respectively. The corresponding experimental ratio La/Fe is almost 1, further demonstrating that pure LaFeO₃ phase was synthesized in perfect agreement with the XRD data.

The specific surface area of nanosized LaFeO₃ particles calculated by the BET method was 38.5 m²/g. However, that of the bulk LaFeO₃ prepared by traditional solid state reaction of La₂O₃ and Fe₂O₃ at high temperature of 1000 °C after a long heating time of 6 h was 4.35 m²/g. The BET specific surface area of the nanosized LaFeO₃ was almost eight times more than that of bulk LaFeO₃ sample. This suggests that the LaFeO₃ nanoparticles have better surface adsorption property. Meanwhile, the high specific surface area of

Table 3The microwave-assisted reduction of various aromatic nitro compounds with 2-propanol over nanosized LaFeO₃ catalyst.^{a,b}

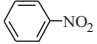
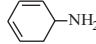

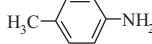
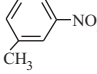
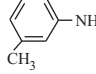
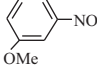
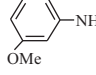
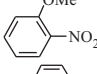
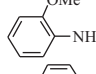
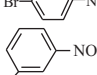
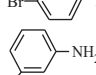
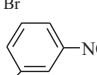
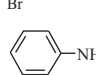
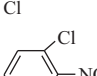
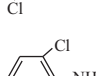
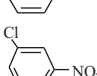
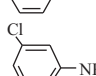
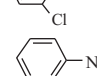
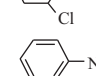
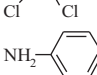
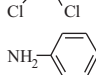
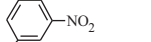
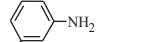
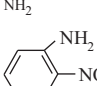
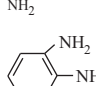
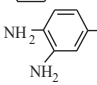
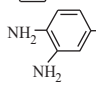
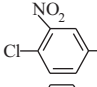
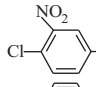
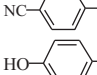
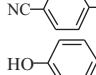
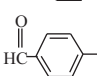
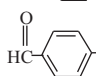
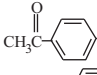
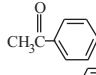
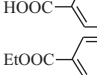
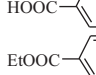
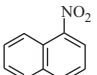
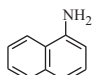






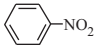
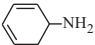
Entry	Nitro compounds	Product	Time (min)	Conversion (%) ^c	Isolated yield (%)
1			18	100	95
2			13	100	98
3			20	98	93
4			8	100	98
5			18	99	93
6			14	100	98
7			19	99	96
8			14	100	98
9			18	99	97
10			16	100	98
11			20	99	94
12			12	99	94
13			16	99	96
14			16	99	95
15			20	82	70
16			10	100	98
17			10	100	98
18			20	97	89
19			15	98	90
20			15	98	93
21			19	99	94
22			18	98	93
23			6	99	95

Table 3 (Continued)

Entry	Nitro compounds	Product	Time (min)	Conversion (%) ^c	Isolated yield (%)
24 ^d			37	96	90

^a Reaction conditions: nitro compound (5 mmol), KOH (5 mmol), catalyst (5 mol%), propan-2-ol (20 mL), under microwave irradiation.

^b In all cases, selectivity was over 99% determined by GC–MS analysis of the crude product mixture.

^c Conversions were determined by GC–MS analysis of the crude product mixture.

^d The reaction was carried out on a 50 mmol scale of nitrobenzene.

Table 4

Comparison the reduction of several aromatic nitro compounds to their corresponding amines with 2-propanol over nanosized- and bulk-LaFeO₃ catalysts.^a

Entry	Nitro compound	Nanosized LaFeO ₃ catalyst		Bulk-LaFeO ₃ catalyst	
		Time (min)	Yield (%) ^b	Time (min)	Yield (%) ^b
1	Nitrobenzene	18	95	45	62
2	4-Bromonitrobenzene	14	98	45	68
3	4-Methylnitrobenzene	13	98	45	65
4	4-Cyanonitrobenzene	10	98	45	60
5	4-Nitrophenol	20	89	45	58

^a Reaction conditions: nitro compound (5 mmol), KOH (5 mmol), catalyst (5 mol%), propan-2-ol (20 mL), under microwave irradiation.

^b Yields are for isolated pure product.

Table 5

Comparison the reduction of nitrobenzene with 2-propanol over various nanosized perovskite-type catalysts.^{a,b}

Entry	Perovskite-type oxide	Time (min)	Conversion (%) ^c	Isolated Yield (%)
1	LaFeO ₃	18	100	95
2	SmFeO ₃	18	99	93
3	NdFeO ₃	20	98	92
4	GdFeO ₃	20	98	92
5	BiFeO ₃	20	99	96
6	LaCoO ₃	35	74	68
7	LaCrO ₃	35	67	60
8	LaMnO ₃	35	65	58

^a Reaction conditions: nitrobenzene (5 mmol), KOH (5 mmol), catalyst (5 mol%), propan-2-ol (20 mL), under microwave irradiation.

^b In all cases, selectivity was over 99% determined by GC–MS analysis of the crude product mixture.

^c Conversions were determined by GC–MS analysis of the crude product mixture

Table 6

Comparison the reduction of several aromatic nitro compounds to their corresponding amines with 2-propanol under microwave and conventional heatings.^{a,b}

Entry	Nitro compound	Microwave method		Conventional method	
		Time (min)	Yield (%) ^c	Time (min)	Yield (%) ^c
1	Nitrobenzene	18	95	240	94
2	4-Bromonitrobenzene	14	98	150	95
3	4-Methylnitrobenzene	13	98	320	93
4	4-Cyanonitrobenzene	10	98	120	96
5	4-Nitrophenol	20	97	160	90
6	4-Nitroacetophenone	15	98	180	92

^a Reaction conditions: nitrobenzene (5 mmol), KOH (5 mmol), catalyst (5 mol%), propan-2-ol (20 mL), under microwave irradiation and conventional heating.

^b In all cases, selectivity was over 99% determined by GC–MS analysis of the crude product mixture.

^c Yields are for isolated pure product.

the nanosized LaFeO₃ product also indicated the possibility of its application as an efficient catalytic material.

3.2. Catalytic activity of LaFeO₃ nanoparticles

The aim of this work was to evaluate the activity of perovskite-type LaFeO₃ nanoparticles as a novel heterogeneous catalyst for the catalytic transfer hydrogenation. The reduction of nitrobenzene with propanol-2-ol was chosen as a model reaction to optimize the reaction conditions. In a typical reaction, a mixture of nitrobenzene (5 mmol) and KOH (5 mmol) in 2-propanol (20 mL) was stirred in the presence of different loadings of nanosized LaFeO₃ catalyst under microwave irradiation (180 W; 20%). The results presented in Table 1. As can be seen, the nitrobenzene conversion and product yield increased with increasing the catalyst amount from 1 to 5 mol% which is due to the proportional increase in the number

of active sites (Table 1, entries 1–3). However, no further improvement was observed with higher loads (Table 1, entries 4 and 5). The optimal catalyst load showed to be 5 mol% which produced aniline as the only product of the reaction in 95% yield after 18 min, without any trace of other by-products. The reduction of nitrobenzene without the LaFeO₃ catalyst or in the absence of KOH failed completely (Table 1, entries 6 and 7), confirming that the catalyst and base are essential for this reaction. No reaction was also observed in the absence of microwave irradiation (Table 1, entry 8).

The influence of alcoholic H-donors such as methanol, ethanol, propan-1-ol, propan-2-ol, butan-2-ol and *tert*-butyl alcohol was also investigated on the reaction. The results in Table 2 show that the best result in terms of reaction time, substrate conversion and product yield have been achieved in the presence of propan-2-ol (Table 2, entry 16). Other alcohols required longer reaction times and gave lower yields (Table 2, entries 2–6). In the presence of

Table 7
Reusability of the nanosized LaFeO₃ catalyst.^a

Run	1	2	3	4
Time (min)	18	18	20	20
Yield (%) ^b	95	94	93	93

^a Reaction conditions: nitrobenzene (5 mmol), KOH (5 mmol), catalyst (5 mol%), propan-2-ol (20 mL) under microwave irradiation. ^b Isolated yields.

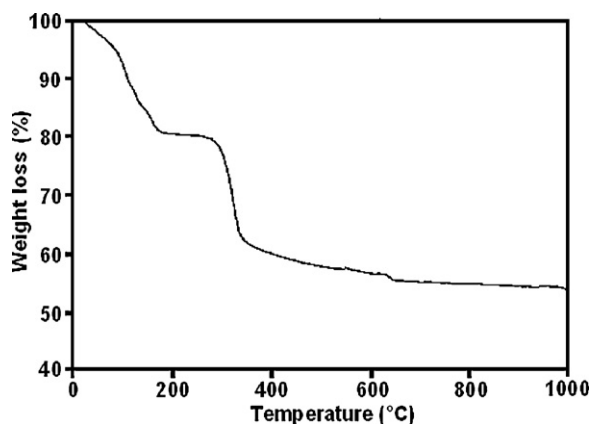


Fig. 1. TGA curve of the La[Fe(CN)₆]·5H₂O complex.

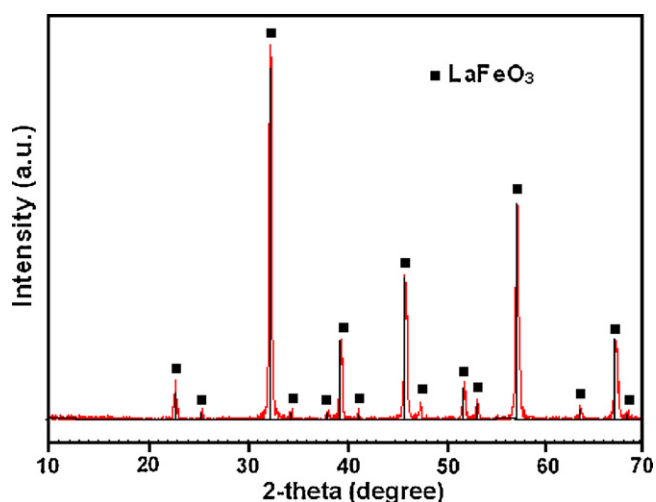


Fig. 2. XRD pattern of the LaFeO₃ nanoparticles.

tert-butyl alcohol which possesses no α -H atom, observable reduction did not occur and the starting nitro compound was recovered unchanged. These findings confirm that the type of alcohol plays an important role in this reaction. Propan-2-ol was the optimal alcohol for the reduction of nitro compounds.

To explore the potential of this catalytic system, the reduction of a variety of aromatic nitro compounds was studied under the optimized reaction conditions. The results in Table 3 show that aromatic nitro compounds containing various electron donating/withdrawing groups were converted to the corresponding amines in excellent yields (>90%) within very short reaction times of 6–20 min in accordance with Scheme 1.

As can be seen in Table 3, electron withdrawing/donating groups do not have a significant influence on the reaction times and yields. In all cases, amines were found to be the only product of the reactions and the usual side products of nitro reduction such as azoxy, azo, and hydrazo compounds were not observed in the final product. The present method was highly chemoselective in the presence

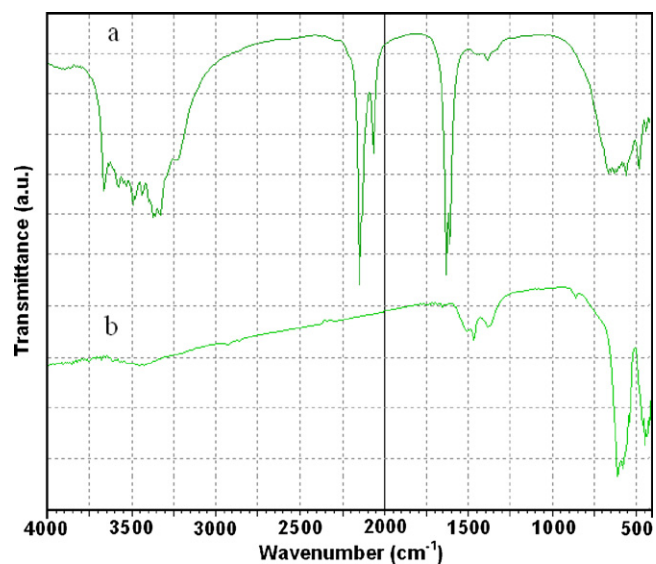


Fig. 3. FT-IR spectra of (a) La[Fe(CN)₆]·5H₂O complex and (b) LaFeO₃ nanoparticles.

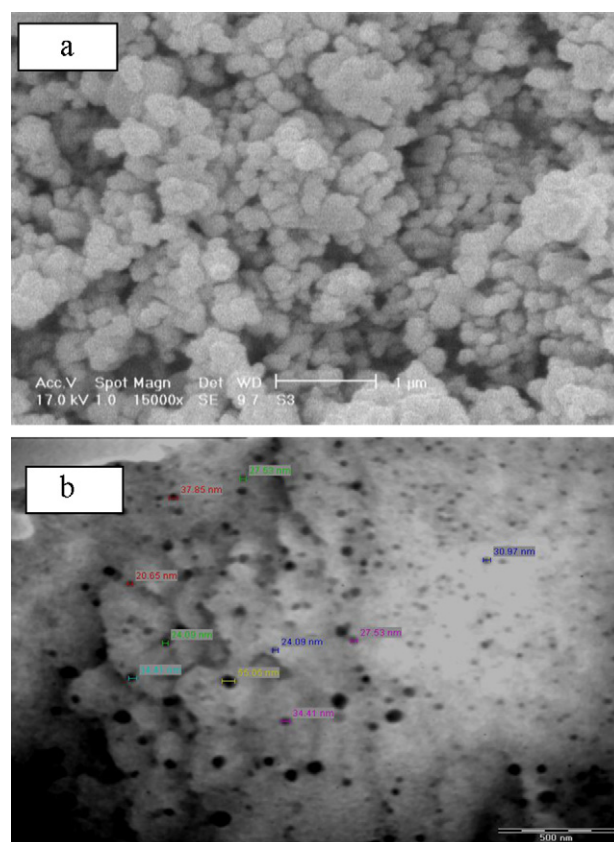


Fig. 4. (a) SEM and (b) TEM images of the LaFeO₃ nanoparticles.

of sensitive functional groups. As can be seen, hydrogenlysable or reducible groups such as halogens, -OH, -NH₂, -OCH₃, -CN, -COMe, -CHO, -COOH and -COOEt were not affected at all under the reaction conditions. Halogenated nitro compounds were reduced to the amino compounds without losing halides (Table 3, entries 6–11). The catalyst also shows promise for regioselective reduction of dinitro compounds, so that selective reduction of a nitro group in presence of the other was accomplished (Table 3, entry 16). Nitro compounds containing carbonyl groups were also reduced to the corresponding amino compounds and the reduction of aldehyde

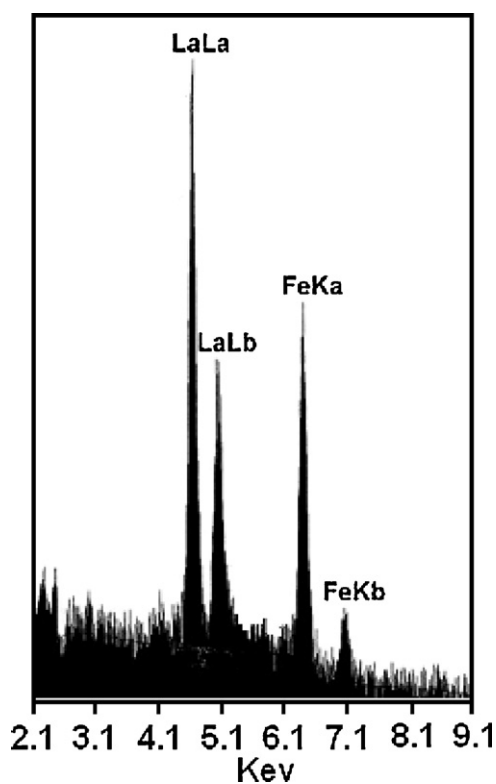
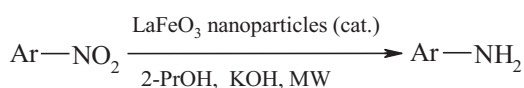


Fig. 5. Energy dispersive X-ray (EDX) spectrum of the LaFeO₃ nanoparticles. Composition (at.%): La = 50.18, Fe = 49.82.



Scheme 1.

functional group and other carbonyl groups to the corresponding alcohols was not observed (Table 3, entries 19–22). Furthermore, this reduction was also successfully carried out on bulkier molecule such as 1-naphthylamine with high yield (Table 3, entry 23). In some cases the activity was significantly influenced by the position of the substituents on the aromatic ring. For example, the presence of a methyl/halide/amine group, *ortho* or *meta* to the nitro group increased the reaction time to a larger extent than at the *para*-position due to steric effects. This new reduction system was easily scaled-up and served for synthesis of aniline at a several gram scale. The reduction of nitrobenzene into aniline was performed on a 50 mmol scale. The yield of product was slightly lower (Table 3, entry 24) comparing to the 5 mmol scale (Table 3, entry 1).

The reduction of several substrates was also investigated over a bulk-sized LaFeO₃ catalyst under the optimized conditions. This sample with an average particle size of 25 μm and BET surface area of 3.5 m²/g, was prepared by classic solid state reaction of La₂O₃ and Fe₂O₃ at 1000 °C. The results in Table 4 clearly indicate that the nanosized LaFeO₃ is much more active than the bulk LaFeO₃ sample. The LaFeO₃ nanoparticles have a large surface to volume ratio and consequently exhibit increased surface activity as compared to bulk sample. It is well known that the higher specific surface area of nanomaterials provides the much higher density of active sites as well as the more contact area between reactants and catalyst to achieve higher efficiency.

The reaction was then studied in the presence of other nanosized perovskite-type oxides. It can be seen in Table 5, Fe(III)-containing perovskite-type oxides such as SmFeO₃, NdFeO₃, GdFeO₃ and

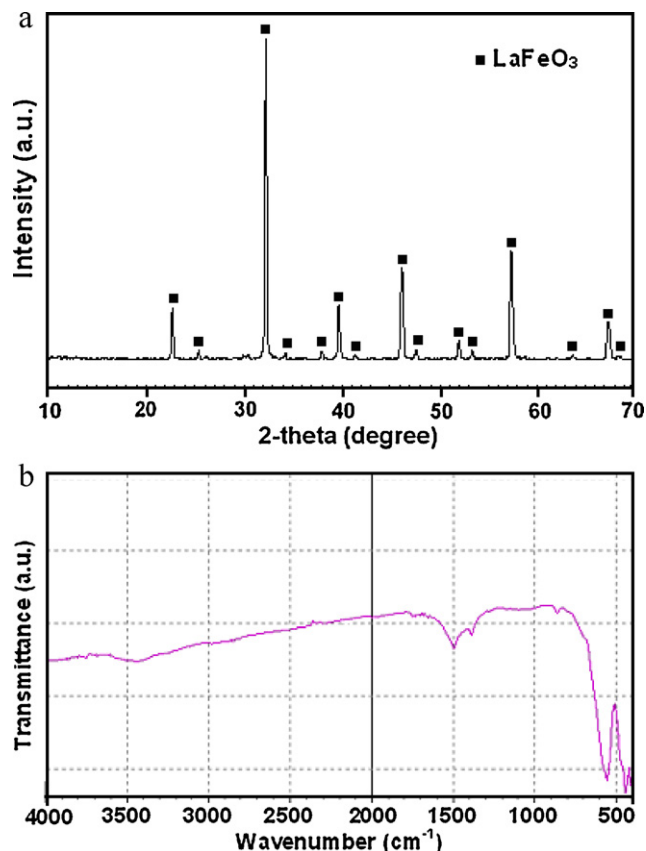
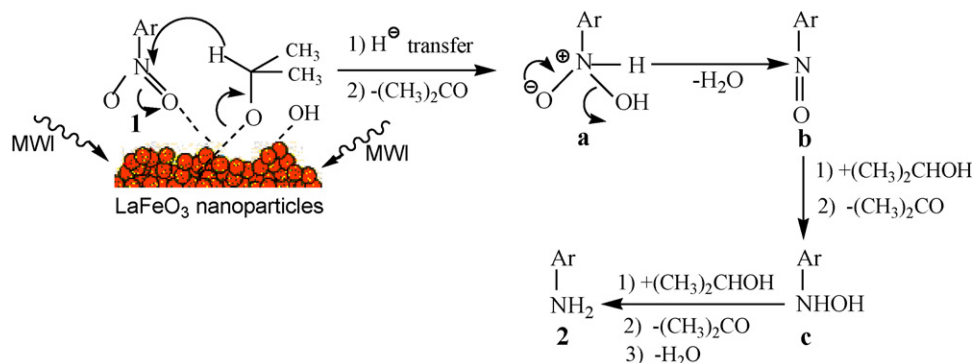


Fig. 6. (a) XRD and (b) FT-IR of the recovered LaFeO₃ catalyst after the fourth run.

BiFeO₃ were almost equally effective in the reaction while LaCoO₃, LaCrO₃ and LaMnO₃ were not effective. This finding confirms that Fe(III) ions in the perovskite-type structure of the catalyst play a vital role in the catalytic reaction.

The reduction of several nitro substrates was also conducted under conventional heating at the same conditions. The results were compared with microwave method in Table 6. As expected, the conventional heating took longer reaction time for the maximum conversion under the same reaction conditions. From this Table, it is evident that the microwave heating dramatically accelerated reaction rate. It is, however, noteworthy here that the corresponding amines were obtained through both conditions. The difference in the reaction times confirms that the heating mechanism is different in these methods.

To demonstrate the recyclability and stability of the catalyst, it was separated at the end of the reduction of nitrobenzene, dried and activated at 200 °C for 1 h. The recovered catalyst was reused in the next run under the same conditions. The results in Table 6 indicate that there is no appreciable difference in the yields after four runs. The recovered LaFeO₃ after the fourth run was characterized by XRD and FT-IR. As shown in Fig. 6, XRD and FT-IR of the recycled LaFeO₃ catalyst did not show significant change in comparison with the fresh catalyst (Figs. 2 and 3). This observation confirms that the LaFeO₃ nanoparticles are stable under the reaction conditions and did not affect by the reactants. This could be attributed to the high stability of the perovskite-type structure of LaFeO₃ nanoparticles which behaves truly as a heterogeneous solid catalyst. On the other hand, no detectable leaching of Fe was observed in the first as well as the fourth run of the reaction by ICP-AES analysis. Also, in an experiment when the catalyst separated from the reaction mixture shortly (8 min) after the beginning microwave irradiation and the reaction filtrate was further irradiated, no extra



Scheme 2. The reduction of nitro aromatic compounds over LaFeO₃ nanoparticles under microwave irradiation (MWI).

formation of amine was observed via GC–MS analysis even after 20 min. These observations confirm that the reaction catalyzed by the LaFeO₃ nanoparticles is heterogeneous in nature.

On the basis of the above observations and previously reported mechanism [33–40], the possible pathway for the reduction of nitroarenes over LaFeO₃ nanoparticles is shown in Scheme 2. As shown in Scheme 2, catalytic reduction is initiated by coordinating the nitro group of the substrate and the hydroxyl group of 2-propanol on the surface of the nanoparticles as Lewis acidic sites. The alcohol molecules can be easily converted to alkoxide species in the presence of KOH base, which are well known activated H-donor. The adsorbed nitro group is attacked by the hydride ion of alcohol, led to the direct hydride transfer from the alcohol to adjacent substrate molecules. Thus, the formation of aniline from nitrobenzene proceeds via the formation of nitrosobenzene (b) and *N*-phenylhydroxylamine (c) as the intermediates. In all reactions, acetone was found by GC–MS analysis which is in consistence with this mechanism. Also, the chemoselective reduction of a nitro group ahead of a carbonyl group can be explained. According to this mechanism, since the nitro group can pull electrons more strongly from the aromatic ring compared to other functional groups, it can easily be adsorbed on the catalyst surface leading to the amine products.

As shown in the above mechanism, LaFeO₃ nanoparticles dispersed in 2-propanol act as a catalyst and provide with their surface as a reaction field. On the basis of the characteristics of our liquid–solid heterogeneous catalytic system, it seems that the phenomenon of “nonequilibrium local heating”, observed by Tsukahara et al. plays a significant role to this microwave-enhanced catalytic reaction [62]. The “nonequilibrium local heating” is defined as the phenomenon of heating domains at much higher temperatures than a bulk solution temperature. This phenomenon was induced only under microwave irradiation but not by conventional heating. LaFeO₃ is a ferromagnetic material with a large magnetic loss so that interacts strongly with the magnetic field of microwave [63–65]. As a result, the temperature of the propan-2-ol molecules should be increased both by the dielectric loss of the propan-2-ol molecules and by the heat transfer from the LaFeO₃ nanoparticles heated through the magnetic interaction with microwave to the solvent. Therefore, the temperature the propan-2-ol molecules in proximity to the surface of the LaFeO₃ nanoparticles went up abruptly under microwave irradiation. For these reasons, the catalytic transfer hydrogenation reaction on the surface of the LaFeO₃ nanoparticles were accelerated under microwave irradiation compared to conventional heating conditions even at the same reaction temperatures. We can suggest that the enhancement in the reduction rate of the aromatic compounds caused by the phenomenon of “nonequilibrium local heating” occurring to the propan-2-ol molecules in proximity of the LaFeO₃ nanoparticles under microwave irradiation. The following facts confirm this suggestion: (a) The present heterogeneous catalytic system is similar

to the catalytic system investigated by Tsukahara et al. (b) LaFeO₃ nanoparticles as ferromagnetic material having strong interaction with the magnetic field of microwave. (c) Further evidence supporting the above suggestion was drawn from the fact that when non-ferrite perovskite-type oxides such as LaCoO₃, LaCrO₃ and LaMnO₃ were used instead of LaFeO₃ catalyst, the efficiency of the reaction decreases (see Table 5). This observation can be related to non-ferromagnetic properties of these perovskite-type oxides which led to weak interaction with microwave irradiation.

4. Conclusions

LaFeO₃ nanoparticles having high specific surface area were readily prepared via thermal decomposition of the La[Fe(CN)₆]₅·5H₂O complex and their catalytic activity was evaluated in the reduction of aromatic nitro compounds to amines using propan-2-ol under microwave irradiation. Under the optimized condition, efficient and selective reduction of aromatic nitro compounds into the corresponding aromatic amines was occurred over recyclable LaFeO₃ nanoparticles catalyst. The advantages of this method are: highly selective reduction of nitro compounds in the presence of other reducible or hydrogenlysable groups, ready availability and ease of operation, rapid reduction, high yields of substituted amines, avoidance of strong acid media, no equipment of pressure apparatus and cost affectivity. The present method is applicable for large scale preparation of different substituted anilines as well as other aryl amines.

Acknowledgments

The authors gratefully acknowledge the Lorestan University Research Council and Iran Nanotechnology Initiative Council (INIC) for their financial support.

References

- [1] G.W. Kabalka, R.S. Verma, in: B.M. Trost, I. Fleming (Eds.), *Comprehensive Organic Synthesis*, 8, Pergamon, Oxford, 1991, pp. 363–379.
- [2] R.C. Larock, *Comprehensive Organic Transformations: A Guide to Functional Group Preparation*, 2nd ed., Wiley-VCH, Weinheim, 1999, 821–828.
- [3] P. Rylander, *Catalytic Hydrogenation in Organic Synthesis*, Academic Press, New York, N.Y., 1979, 114–134.
- [4] M. Hudlicky, *Reductions in Organic Chemistry*, 2nd ed., ACS Monograph, 1996.
- [5] C.A. Marlic, S. Motamed, B. Quinn, *J. Org. Chem.* 60 (1995) 3365–3369.
- [6] K.M. Doozee, M. Figel, K.D. Stewart, J.W. Canary, C.B. Knobler, D.J. Cram, *J. Am. Chem. Soc.* 109 (1987) 3098–3107.
- [7] Al/NH₄Cl/MeOH D. Nagaraja, M.A. Pasha, *Tetrahedron Lett.* 40 (1999) 7855–7856.
- [8] Zn/CaCl₂/EtOH R. Shundberg, W. Pitts, *J. Org. Chem.* 56 (1991) 3048–3054.
- [9] Co₂(CO)₈/H₂O H.Y. Lee, M. An, *Bull. Korean Chem. Soc.* 25 (2004) 1717–1719.
- [10] Mo(CO)₆ S. Iyer, G.M. Kulkarni, *Synth. Commun.* 34 (2004) 721–725.
- [11] SnCl₂/ionic liquid P. De, *Synlett Lett.* (2004) 1835–1837.
- [12] N₂H₄/FeCl₃ A. Vass, J. Dudar, R.S. Varma, *Tetrahedron Lett.* 42 (2001) 5347–5379.

- [13] N_2H_4/Zn S. Gowda, D.C. Gowda, *Ind. J. Chem.* 42B (2003) 180–183.
- [14] $TiCl_3$ J. George, S. Chandrasekaran, *Synth. Commun.* 13 (1983) 495–499.
- [15] $NaH_2PO_2/FeSO_4$ H.M. Meshram, Y.S.S. Ganesh, K.C. Sekhar, J.S. Yadav, *Synlett Lett.* (2000) 993–994.
- [16] $HCOONH_4/Mg$ G.R. Srinivasa, K. Abiraj, D.C. Gowda, *Ind. J. Chem.* 42B (2003) 2885–2887.
- [17] $HCOON_2H_5/Zn$ S. Gowda, B.K.K. Gowda, D.C. Gowda, *Synth. Commun.* 33 (2003) 281–289.
- [18] $HCOOH/Raney$ nickel D.C. Gowda, A.S.P. Gowda, A.R. Baba, *Synth. Commun.* 30 (2000) 2889–2895.
- [19] $N_2H_4/Raney$ nickel F. Yuste, M. Saldana, F. Walls, *Tetrahedron Lett.* 23 (1982) 147–148.
- [20] $HCOONa/K_3PO_4$ J.H. Babler, S.J. Sarussi, *Synth. Commun.* 11 (1981) 925–930.
- [21] $N_2H_4/AlH_3/AlCl_3$ B.M. Adger, R.G. Young, *Tetrahedron Lett.* 25 (1984) 5219–5222.
- [22] $N_2H_4 \cdot H_2O/Fe_2O_3/MgO$ P.S. Kumbhar, J.S. Valnte, F. Figueras, *Tetrahedron Lett.* 39 (1998) 2573–2574.
- [23] Na_2S/NEt_4Br G.D. Yadav, S.V. Lande, *Adv. Synth. Catal.* 347 (2005) 1235–1241.
- [24] Sm/NH_4Cl /ultrasound irradiation M.K. Basu, F.F. Becker, B.K. Banik, *Tetrahedron Lett.* 41 (2000) 5603–5606.
- [25] $HCOON_2H_5/Raney$ Ni S. Gowda, D.C. Gowda, *Gowda Tetrahedron Lett.* 58 (2002) 2211–2213.
- [26] HI J.S.D. Kumar, M.M. Ho, T. Toyokuni, *Tetrahedron Lett.* 42 (2001) 5601–5603.
- [27] $S_8/NaHCO_3$ M.A. McLaughlin, D.M. Barnes, *Tetrahedron Lett.* 41 (2001) 5347–5349.
- [28] $NaBH_4/Raney$ nickel I. Pogorelic, M. Filipan-Litvic, S. Merkas, G. Ljubic, L. Cepanec, M. Litvic, *J. Mol. Catal. A: Chem.* 274 (2007) 202–207.
- [29] $Fe(acac)_3/TMDS$ L. Pehlivan, E. Metay, S. Laval, W. Dayoub, P. Demonchaux, G. Mignani, M. Lemaire, *Tetrahedron Lett.* 51 (2010) 1939–1941.
- [30] $SnCl_2$ /ultrasound irradiation A.B. Gamble, J. Garner, C.P. Gordon, S.M.J. O'Conner, P.A. Keller, *Synth. Commun.* 37 (2007) 2777–2786.
- [31] R.A.W. Johnstone, A.H. Wilby, I.D. Entwistle, *Chem. Rev.* 85 (1985) 129–170.
- [32] D.C. Gowda, B. Mahesha, *Synth. Commun.* 30 (2000) 3639–3644.
- [33] S.K. Mohapatra, S.U. Sonavane, R.V. Jayaram, P. Selvam, *Tetrahedron Lett.* 43 (2002) 8527–8529.
- [34] S.K. Mohapatra, S.U. Sonavane, R.V. Jayaram, P. Selvam, *Org. Lett.* 24 (2002) 4297–4300.
- [35] S.U. Sonavane, R.V. Jayaram, *Synth. Commun.* 33 (2003) 843–849.
- [36] S.U. Sonavane, S.K. Mohapatra, R.V. Jayaram, P. Selvam, *Chem. Lett.* 32 (2003) 142–143.
- [37] S.K. Mohapatra, S.U. Sonavane, R.V. Jayaram, P. Selvam, *Appl. Catal. B: Environ.* 46 (2003) 155–163.
- [38] S.U. Sonavane, R.V. Jayaram, *Synlett Lett.* (2004) 146–148.
- [39] P. Selvam, S.U. Sonavane, S.K. Mohapatra, R.V. Jayaram, *Tetrahedron Lett.* 45 (2004) 3071–3075.
- [40] P. Selvam, S.U. Sonavane, S.K. Mohapatra, R.V. Jayaram, *Adv. Synth. Catal.* 346 (2004) 542–544.
- [41] H. Wen, K. Yao, Y. Zhang, Z. Zhou, A. Kirschning, *Catal. Commun.* 10 (2009) 1207–1211.
- [42] Y. Chen, J. Qiu, X. Wan, J. Xiu, *J. Catal.* 242 (2006) 227–230.
- [43] P.S. Kumbhar, J. Sanchez-Valente, J.M.M. Millet, F. Figueras, *J. Catal.* 191 (2000) 467–473.
- [44] M. Kumarraja, K. Pitchumani, *Appl. Catal. A: Gen.* 265 (2004) 135–139.
- [45] G. Schmidt, *Nanoparticles: From Theory to Application*, VCH, Weinheim, 2004.
- [46] B. Zhou, S. Han, R. Raja, G.A. Somorjai, *Nanotechnology in Catalysis*, 3, Springer, 2007.
- [47] M.F.M. Zwinkels, S.G. Jaras, P.G. Menon, T.A. Griffin, *Catal. Rev. Sci. Eng.* 35 (1993) 319–358.
- [48] K.S. Song, H.X. Cui, S.D. Kim, S.K. Kang, *Catal. Today* 47 (1999) 155–160.
- [49] M. O'Connell, A.K. Norman, C.F. Huttermann, M.A. Morris, *Catal. Today* 47 (1999) 123–132.
- [50] P. Ciambelli, S. Cimino, S. De Rossi, L. Lisi, G. Minelli, P. Porta, G. Russo, *Appl. Catal. B: Environ.* 29 (2001) 239–250.
- [51] R. Spinicci, M. Faticanti, P. Marini, S. De Rossi, P. Porta, *J. Mol. Catal. A: Chem.* 197 (2003) 147–155.
- [52] N. Russo, D. Fino, G. Saracco, V. Specchia, *J. Catal.* 229 (2005) 459–469.
- [53] F. De Bruijn, *Green Chem.* 7 (2005) 132–150.
- [54] S. Farhadi, N. Rashidi, *Polyhedron* 29 (2010) 2959–2965, and references cited therein.
- [55] S. Farhadi, M. Zaidi, *J. Mol. Catal. A: Chem.* 299 (2009) 18–25.
- [56] S. Farhadi, M. Zaidi, *Appl. Catal. A: Gen.* 354 (2009) 119–126.
- [57] S. Farhadi, S. Sepahvand, *J. Mol. Catal. A: Chem.* 318 (2010) 75–84.
- [58] S. Farhadi, S. Panahandehjoo, *Appl. Catal. A: Gen.* 382 (2010) 293–302.
- [59] H.P. Klug, L.E. Alexander, *X-ray Diffraction Procedures*, 2nd ed., Wiley, New York, 1964.
- [60] K. Nakamoto, *Infrared and Raman Spectra of Inorganic and Coordination Compounds, Part B: Applications in Coordination Organometallic, and Bioinorganic Chemistry*, 6th ed., Wiley, New York, 2009.
- [61] G.V.S. Rao, C.N.R. Rao, J.R. Ferraro, *Appl. Spectrosc.* 24 (1970) 436–445.
- [62] Y. Tsukahara, A. Higashi, T. Yamauchi, T. Nakamura, M. Yasuda, A. Baba, Y. Wada, *J. Phys. Chem. C* 114 (2010) 8965–8970.
- [63] P. Monica, M. Jose, M. Calderon, *J. Alloys Compd.* 509 (2011) 4108–4116.
- [64] M. Rajendran, A.K. Bhattacharya, *J. Eur. Ceram. Soc.* 26 (2006) 3675–3679.
- [65] S. Hui, X.U. Jiayue, W.U. Anhua, *J. Rare Earths* 28 (2010) 416–419.